the FEBS Journal

A high molecular mass zinc transporter MTP12 forms a functional heteromeric complex with MTP5 in the Golgi in *Arabidopsis thaliana*

Takashi Fujiwara[1], Miki Kawachi[1], Yori Sato[1], Haruki Mori[1], Natsumaro Kutsuna[2,3], Seiichiro Hasezawa[2] and Masayoshi Maeshima[1]

1 Laboratory of Cell Dynamics, Graduate School of Bioagricultural Sciences, Nagoya University, Japan
2 Department of Integrated Biosciences, The University of Tokyo, Japan
3 LPixel Inc., Bunkyo-ku, Japan

Keywords
Arabidopsis; cation diffusion facilitator; Golgi; MTP; zinc

Correspondence
M. Maeshima, Laboratory of Cell Dynamics, Graduate School of Bioagricultural Sciences, Nagoya University, Furo-cho, Chikusa-ku, Nagoya 464-8601, Japan
Tel: +81 52 789 4096
E-mail: maeshima@agr.nagoya-u.ac.jp

(Received 4 October 2014, revised 31 January 2015, accepted 26 February 2015)

doi:10.1111/febs.13252

Zinc (Zn) is an essential micronutrient required for plant growth and development. In *Arabidopsis thaliana*, several families of Zn transporters engaged in Zn import, export and intracellular compartmentalization play important roles in Zn homeostasis. We describe a novel Zn transporter, *A. thaliana* metal tolerance protein 12 (AtMTP12), which belongs to the cation diffusion facilitator family. AtMTP12 is predicted to consist of 798 amino acids and have 14 transmembrane segments. The expression of AtMTP12 in suspension-cultured cells was not affected by Zn deficiency or excess. Heterologous expression in a mutant of budding yeast (*Saccharomyces cerevisiae*) that lacks Msc2p, an orthologue of AtMTP12, revealed that AtMTP12 complements the growth phenotype of the *msc2* mutant when AtMTP5t1, one of the splicing variants of AtMTP5, is coexpressed. Transient expression of AtMTP12-fused green fluorescent protein in *A. thaliana* mesophyll protoplasts demonstrated that AtMTP12 is localized to the Golgi apparatus. Moreover, AtMTP12 and AtMTP5t1 interact in the Golgi, as determined by a bimolecular fluorescence complementation assay. These results suggest that AtMTP12 forms a functional complex with AtMTP5t1 to transport Zn into the Golgi.

Database
Nucleotide sequence data for full-length of *AtMTP12* is available in the DDBJ/EMBL/GenBank database under accession number AB986563.

Introduction

Zn is an essential micronutrient for plant growth, playing crucial roles as a catalytic or structural cofactor in many enzymes and regulatory proteins [1]. More than 1200 proteins are predicted to contain, bind or transport Zn in *A. thaliana* [2]. Despite its importance, excess Zn can be toxic because Zn competes with other metal ions for the same binding sites of proteins, leading to their becoming inactive [1]. Thus, Zn must be kept at appropriate concentrations in the cell and properly distributed in each

Abbreviations
3HA, three tandem hemagglutinin; CaMV, cauliflower mosaic virus; CDF, cation diffusion facilitator; CSD, copper/zinc superoxide dismutase; ER, endoplasmic reticulum; GFP, green fluorescent protein; HMA, heavy metal ATPase; mRFP, monomeric red fluorescent protein; MTP, metal tolerance protein; NosT, nopaline synthase terminator; PIP, plasma membrane intrinsic protein; TGN, *trans*-Golgi network; TM, transmembrane segment; YFP, yellow fluorescent protein; YPGE, YP medium supplemented with glycerol and ethanol; ZIP, zinc-regulated transporter/iron-regulated transporter-like protein.

intracellular compartment. Plants have developed a multiplicity of Zn transport machineries such as Zn-regulated transporter/iron-regulated transporter-like protein (ZIP), heavy metal ATPase (HMA) and metal tolerance protein (MTP) to maintain Zn homeostasis.

Members of the ZIP family transport metal ions from extracellular fluid or intracellular compartments into the cytosol, and members of the HMA and MTP families translocate metal ions in the opposite direction. Among the ZIP members in *A. thaliana*, AtIRT1, AtIRT3 and AtZIP2 have been demonstrated to transport Zn and be localized to the plasma membrane [3–7]. AtZIP1 and AtIRT2, which are localized to the vacuolar membrane and membrane of other intracellular compartment, respectively, also complement a Zn-uptake-deficient yeast mutant [6–8]. However, their physiological roles in Zn homeostasis *in planta* are unknown. By contrast, AtHMA2 and AtHMA4 transport Zn across the plasma membrane and play a key role in xylem loading of Zn for root-to-shoot translocation [9–11]. AtHMA3 is involved in Zn detoxification via transporting Zn into the vacuole. Interestingly, the *AtHMA3* gene from the Columbia strain has a single base-pair deletion, resulting in loss of function of AtHMA3 by truncation of its C terminus [9,12].

The MTP family in *A. thaliana* consists of 12 members. Four members, AtMTP1 to AtMTP4, form a phylogenic subgroup [13]. AtMTP1 and AtMTP3 transport Zn and are localized to the vacuolar membrane [14–16]. Loss-of-function mutants of AtMTP1 show hypersensitivity to excess Zn and high-level expression of *MTP1* enhances tolerance to excess Zn in plants [17–19]. Similar phenomena have been observed for the knockdown and overexpression of *AtMTP3* [15]. These reports indicate that AtMTP1 and AtMTP3 have essential roles in the detoxification of excess Zn. However, *AtMTP1* and *AtMTP3* are different in spatial expression pattern and in response to excess Zn [15,19]. Four other members, AtMTP8 to AtMTP11, are predicted to form another subgroup in the phylogenetic tree [13]. The *AtMTP11* gene reportedly encodes a manganese (Mn) transporter and confers tolerance to excess Mn [20,21].

MTP proteins belong to the cation diffusion facilitator (CDF) family, and most CDF members possess six putative transmembrane segments (TMs). In addition, four members, AtMTP1 to AtMTP4, have a long histidine (His)-rich region between TM4 and TM5. This His-rich region is predicted to act as a Zn-binding pocket and a sensor of Zn levels in the cytosol [16,22]. The *Escherichia coli* Zn transporter YiiP, which is an orthologue of AtMTP1 but lacks the His-rich region, has been well characterized in terms of its higher order structure and Zn transport mechanism at the atomic level [23,24]. These MTP1-related proteins have six TMs and a relatively large C-terminal domain, and form a heterodimer that functions as a Zn^{2+}/H^{+} exchanger.

We focused on AtMTP12, because this protein has unique structural characteristics. AtMTP12 appears to have approximately twice the length of primary sequence as the other AtMTPs. AtMTP12 has been estimated to consist of 798 amino acid residues based on the genomic sequence (At2g04620), whereas AtMTP1 consists of 398 residues. Over the last decade, Zn transporters localized to the vacuolar or plasma membrane have been reported in several plant species [1]. Zn homeostasis must be maintained by cooperative regulation of a large number of Zn transporters in the cell, including those in the endoplasmic reticulum (ER), Golgi apparatus, secretory vesicles, mitochondria and chloroplasts. Therefore, the biochemical and physiological properties of these Zn transporters should be revealed for a good understanding of Zn homeostasis in plants. In this study, we focused on a high molecular mass MTP member, AtMTP12, and investigated its biochemical properties, expression pattern, Zn transport activity and intracellular localization. We revealed that AtMTP12 exists as a full-length protein and is localized to the Golgi membrane. Furthermore, we demonstrated the formation of a heteromeric functional complex of AtMTP12 with another MTP member. Based on these observations, we discuss the biochemical and physiological role of AtMTP12.

Results

Identification of *AtMTP12* cDNA

To isolate full-length *AtMTP12* cDNA, we performed 5′- and 3′-RACE. The ATG at position +84 was assumed to initiate an ORF encoding AtMTP12, consisting of 798 amino acid residues. The programs SOSUI (http://bp.nuap.nagoya-u.ac.jp/sosui/) and TMHMM (http://www.cbs.dtu.dk/services/TMHMM/) predicted that AtMTP12 possesses 14 TMs with cytosolic N and C termini. In addition to an archetypical CDF structure with six TMs in the C-terminal half, AtMTP12 has an exceptionally long N-terminal sequence with eight extra TMs that shows little homology to known proteins. AtMTP12 also contains a His-rich region between TM12 and TM13 (data not shown).

AtMTP12 protein is expressed constitutively in T87 cells

To detect AtMTP12 protein, we generated transgenic T87 cells that express *AtMTP12–3HA* (three tandem hemagglutinin) under the control of the *AtMTP12* promoter. We first confirmed the presence of the transgene in transgenic T87 cells at the DNA level (Fig. 1A). AtMTP12–3HA protein was immunochemically detected in the crude membrane fraction (Fig. 1B), but not in the soluble fractions (data not shown). The apparent molecular mass of AtMTP12–3HA was 82.0 kDa, although the ORF of *AtMTP12–3HA* was predicted to encode a protein of 94.7 kDa.

We next determined the accumulation level of AtMTP12–3HA in transgenic T87 cells treated with various concentrations of Zn for 2 days. The abundance of AtMTP12–3HA in the cells was largely unchanged (Fig. 1C). A time course experiment under Zn-deficient (5 μM *N*,*N*,*N*′,*N*′-tetrakis(2-pyridylmethyl)ethylenediamine) and Zn-excess (500 μM Zn^{2+}) conditions showed that the level of AtMTP12–3HA protein was stable (Fig. 1D). We verified the mRNA expression levels of *AtZIP4* and *AtCSD2* (copper/zinc superoxide dismutase 2) as positive indicators of the effect of Zn deficiency and excess, respectively (Fig. 1E) [19,25]. These results indicate that AtMTP12 accumulation does not depend on Zn concentration. We infer that AtMTP12 is a constitutive component of cells.

AtMTP12 complements *msc2* mutant growth phenotype when AtMTP5t1 is coexpressed

To assess whether AtMTP12 functions as a Zn transporter, we first expressed *AtMTP12* under the control of *TDH3* (GAPDH) promoter in *S. cerevisiae* strain BJ5458 lacking two vacuolar Zn transporters, Zrc1p and Cot1p, both of which confer tolerance to excess Zn [26,27]. This double-mutant is unable to grow in Zn^{2+} concentrations of 0.2 mM or higher. The double-mutant transformed with expression vector pKT10 harboring the *AtMTP1* ORF was used as a positive control [16]. Nevertheless, AtMTP12 did not restore growth in 0.2 mM Zn^{2+} (Fig. 2).

Orthologues to AtMTP12 have been found in humans (*Homo sapiens*, ZnT5), *S. cerevisiae* (Msc2p) and fission yeast (*Schizosaccharomyces pombe*, Cis4). Given that ZnT5, Msc2p and Cis4 respectively form heteromeric complexes with ZnT6, Zrg17p and Zrg17, which are other CDF members [28–30], we hypothesized that AtMTP12 interacts with another CDF member to form a functional complex. A heterologous

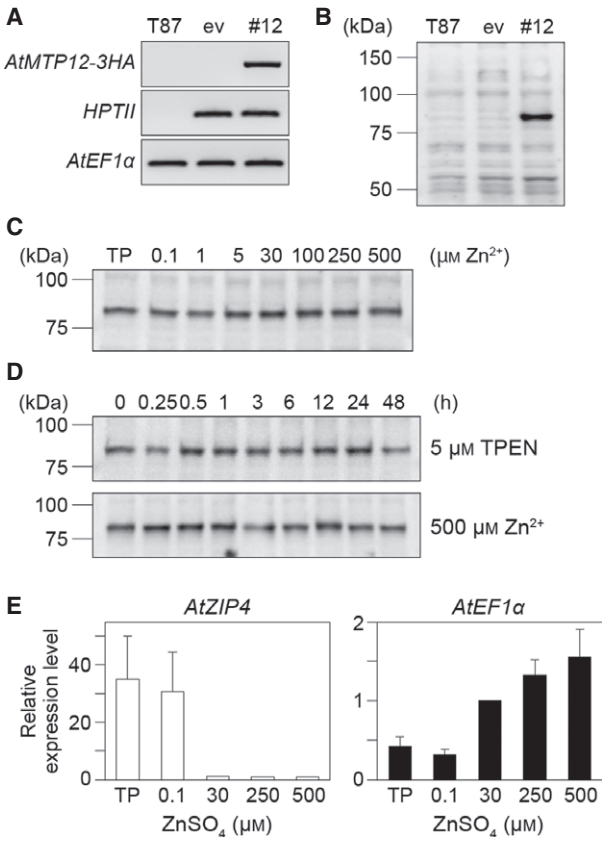

Fig. 1. Expression analysis of AtMTP12–3HA in T87 cells. (A) Analysis of transgenes in T87 cells. The presence of transgenes *AtMTP12–3HA* and *HPTII* (hygromycin phosphotransferase II) was confirmed by PCR using genomic DNA extracted from T87 (T87), T87 transformed with empty vector pCAMBIA35N (ev) and T87 transformed with an *AtMTP12* promoter : *AtMTP12–3HA* construct (#12). *AtEF1α* (elongation factor 1 alpha) was used as a control. (B) Detection of AtMTP12–3HA protein. Crude membrane fractions were prepared from 7-day-old T87 or transgenic T87 cells grown under normal conditions and 15 μg of protein was immunoblotted with anti-HA Ig. The sizes of standard proteins are shown on the left in kDa. (C,D) Changes in AtMTP12–3HA protein levels in response to Zn deficiency or excess. Zn treatment was performed as described in Experimental Procedures. T87 cells were exposed to Zn stress for 2 days (C) or the indicated periods (D). TPEN (D) or TP (E) represents 5 μM *N*,*N*,*N*′,*N*′-tetrakis(2-pyridylmethyl) ethylenediamine. A 15 μg aliquot of crude membrane protein was immunoblotted with anti-HA Ig. (E) Expression patterns of *AtZIP4* and *AtCSD2* mRNA. Transcript levels of *AtZIP4* and *AtCSD2* in T87 cells treated with various concentrations of Zn^{2+} for 2 days were assessed by semi-quantitative RT-PCR as representing a Zn deficiency and excess response gene, respectively. *AtEF1α* was used as an internal control to normalize for variation in the amount of cDNA template. Data show the mean of relative values with one unit being 30 μM $ZnSO_4$ ± SD of three experiments.

expression system of *S. cerevisiae* strain DY150 *msc2* was used to test this hypothesis. The *msc2* mutant grows at 30 °C in rich YP medium supplemented with

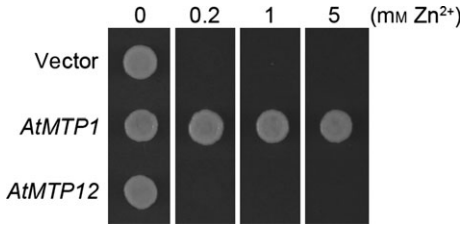

Fig. 2. Complementation analysis of *S. cerevisiae* mutant BJ5458 *zrc1 cot1*. The *zrc1 cot1* double-mutant was transformed with empty vector pKT10 (negative control), *AtMTP1*–pKT10 (positive control) or *AtMTP12*–pKT10. Yeast cells were grown in liquid HC-U medium for 18 h at 30 °C and diluted to 0.1 at D_{660} in the same medium. A 5 μL aliquot of suspension culture was applied to HC-U plates supplemented with the indicated concentrations of $ZnCl_2$. The plates were incubated for 2 days at 30 °C.

glycerol and ethanol (YPGE), but is unable to grow at 37 °C. This growth defect at elevated temperatures is attenuated by addition of Zn [31]. We verified that this growth defect phenotype was still observed even in the presence of galactose in YPGE medium (YPGEgal) at 37 °C (Fig. 3A). However, galactose alleviated this growth defect to some extent, because the *msc2* mutant could grow partially in YPGEgal medium with lower concentrations of Zn than in YPGE medium (data not shown). As a control, the *msc2* mutant was transformed with expression vectors pAUR123GAL1 and pYES2 harboring the *MSC2* ORF to express it under the control of the *GAL1* promoter. The transformed yeast cells grew normally in YPGEgal medium at 37 °C even in the absence of a Zn supply, indicating that these expression vectors are functional in this mutant (Fig. 3A). Thus, we inserted the *AtMTP12* ORF into pAUR123GAL1 and the ORFs of the other MTP members into pYES2. With regard to *AtMTP3*, *AtMTP5*, *AtMTP6* and *AtMTP9*, the existence of splicing variants is reported in the database of The Arabidopsis Information Resource (TAIR; http://blast.jcvi.org/euk-blast/plantta_blast.cgi). We cloned each variant and referred to them as *t1* and *t2* (e.g. *AtMTP3t1* and *AtMTP3t2*). A growth assay showed that *msc2* cells expressing *AtMTP12* alone were unable to grow in YPGEgal medium at 37 °C (Fig. 3B). Even in the presence of high concentrations of Zn in YPGEgal medium, *AtMTP12*-expressing *msc2* cells grew no better than the *msc2* cells transformed with empty vectors (data not shown). However, when *AtMTP12* was coexpressed with *AtMTP5t1*, growth was significantly recovered in YPGEgal medium supplemented with 25 μM Zn^{2+} (Fig. 3B). Yeast cells expressing both *AtMTP12* and *AtMTP5t1* still grew better than cells transformed with empty vectors when grown in the presence of higher concentrations of Zn^{2+} (data not shown). AtMTP5t1 alone could not complement the growth defect in YPGEgal medium (Fig. 3B). We also found that AtMTP1, AtMTP3t1 and AtMTP4 were able to restore growth even in the absence of *AtMTP12*. These results suggested that AtMTP12 and AtMTP5t1 form a functional complex to mediate Zn transport.

We also applied this double gene expression system to a BJ5458 *zrc1 cot1* double-mutant. ORFs of *AtMTP12* and the other MTP members were ligated into pAUR123 and pKT10 vectors to be expressed under the control of the *ADH1* and *TDH3* promoter, respectively. The double-mutant cells expressing both *AtMTP12* and *AtMTP5t1* or *AtMTP5t1* alone grew poorly in medium supplemented with 0.2 mM Zn^{2+}, like the double-mutant transformed with empty vectors (Fig. 4). By contrast, growth of yeast cells expressing *AtMTP1*, *AtMTP2*, *AtMTP3t1*, *AtMTP3t2* or *AtMTP4* was not affected by excess Zn regardless of the presence of AtMTP12 (Fig. 4). In comparison with AtMTP1, AtMTP2 and AtMTP3t2, a reduced level of Zn tolerance was conferred by AtMTP3t1 and AtMTP4.

AtMTP12 and AtMTP5s are colocalized in the Golgi apparatus

Yeast complementation tests disclosed the AtMTP5t1-dependent Zn transport activity of AtMTP12. We next addressed the question of whether AtMTP12 and AtMTP5t1 are localized to the same membrane. To answer this, chimeric genes *AtMTP12–GFP* and *AtMTP5s–GFP* were transiently and individually expressed in *A. thaliana* mesophyll protoplasts under the control of the cauliflower mosaic virus (CaMV) 35S promoter. Five monomeric red fluorescent protein (mRFP)-tagged intracellular marker genes were expressed simultaneously with *AtMTP12–GFP* and *AtMTP5s–GFP*. Observation using a confocal laser scanning microscope demonstrated that AtMTP12–GFP-dependent green fluorescence appeared as a punctate structure (Fig. 5A). The punctate fluorescence of AtMTP12–GFP clearly overlapped with that of *cis*-Golgi marker mRFP–SYP31 but not with ER marker sp-mRFP–HDEL, *trans*-Golgi network (TGN) marker mRFP–SYP61, or early endosome marker mRFP–ARA7 (Fig. 5A,B). In mesophyll protoplasts expressing *AtMTP12–GFP* and *trans*-Golgi marker *ST–mRFP*, we found several dots in which fluorescence of green fluorescent protein (GFP) and mRFP were located side by side with partial overlap (Fig. 5A, C). These data demonstrated that AtMTP12 is

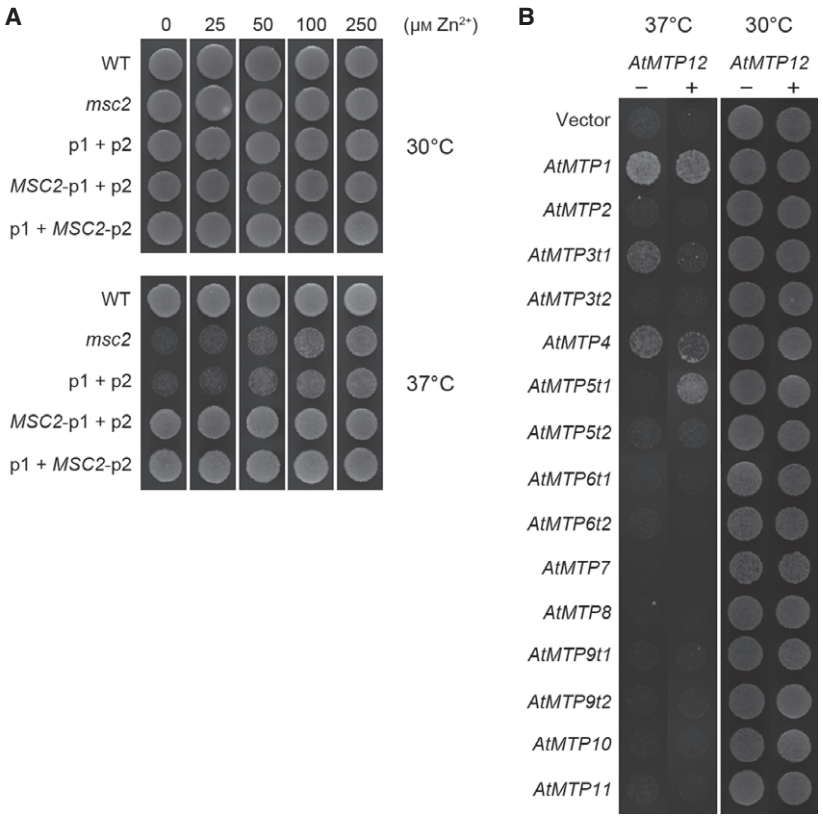

Fig. 3. Complementation analysis of *S. cerevisiae* mutant DY150 *msc2*. (A) Growth assay of *msc2* mutant in YPGEgal medium. The *msc2* mutant was transformed with pAUR123GAL1 (p1), *MSC2*–pAUR123GAL1 (*MSC2*–p1), pYES2 (p2) and *MSC2*–pYES2 (*MSC2*–p2) in the following conbinations: p1 + p2, *MSC2*–p1 + p2 and p1 + *MSC2*–p2. Wild-type (DY150) and transformed yeast cells were grown in liquid SRaf medium with appropriate amino acids for auxotrophy and antibiotics for 18 h at 30 °C and diluted to 0.1 at D_{660} with SGal medium with appropriate amino acids. After incubation at 30 °C for 1 h, volumes of 5 μL were plated onto YPGEgal plates containing the indicated amount of $ZnSO_4$. The plates were incubated for 3 days at 30 or 37 °C. (B) Growth assay of *msc2* mutant expressing *AtMTP*s. The *msc2* cells carrying pAUR123GAL1 (–) or *AtMTP12*-pAUR123GAL1 (+) were transformed with empty vector pYES2 or pYES2 harboring *AtMTPX* ORF. The yeast suspension cultures were prepared as described above and 5 μL was spotted onto YPGEgal plates supplemented with 25 μM $ZnSO_4$. The plates were incubated for 3 days at 30 or 37 °C.

localized to the Golgi apparatus. However, the fluorescence intensity profile revealed that the intensity curve of GFP fitted well with that of mRFP–SYP31 (*cis*-Golgi) compared with ST–mRFP (*trans*-Golgi) (Fig. 5B,C), suggesting that AtMTP12 is enriched in the *cis*-Golgi. The transformed mesophyll protoplasts also displayed a punctate pattern of green fluorescence of GFP-tagged AtMTP5t1 and AtMTP5t2 (Fig. 5D, E). However, unlike AtMTP12, a portion of the AtMTP5s–GFP signal colocalized with mRFP–SYP31 (*cis*-Golgi), and a portion colocalized with ST–mRFP (*trans*-Golgi) (Fig. 5D,E). With regard to other intracellular markers, punctate patterns of AtMTP5s–GFP were obviously separated from patterns of sp-mRFP–HDEL (ER), mRFP–SYP61 (TGN) and mRFP–ARA7 (early endosome). These results suggest that AtMTP5t1 and AtMTP5t2 are localized both to the *cis*- and *trans*-Golgi. Similar results were obtained for the GFP–AtMTP12 and GFP–AtMTP5s fusion proteins (data not shown). By contrast, in mesophyll protoplasts expressing *GFP* alone, green fluorescence was observed in the cytosol and nucleus (data not shown). These results indicate that AtMTP12 and AtMTP5t1 are colocalized in the Golgi.

AtMTP12 and AtMTP5 form a complex in the Golgi apparatus

Next, we tested the interaction between AtMTP12 and AtMTP5s *in vivo* using bimolecular fluorescence complementation analysis. cDNAs of the N-terminal fragment of yellow fluorescent protein (*nYFP*) and

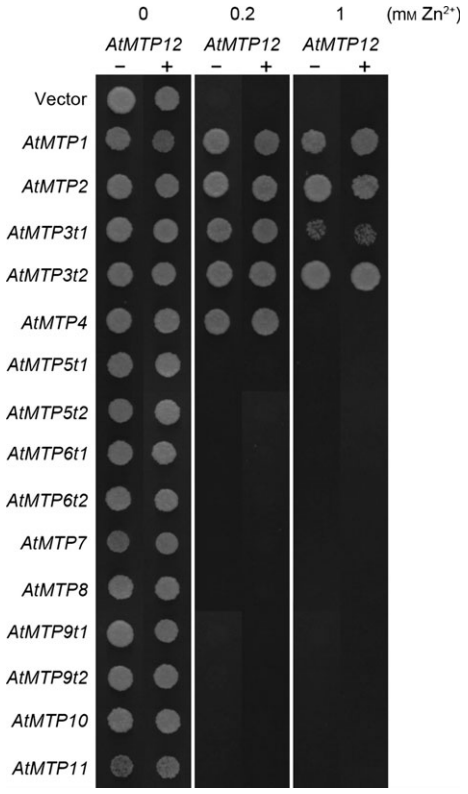

Fig. 4. Growth of *S. cerevisiae* mutant BJ5458 *zrc1 cot1* expressing *AtMTP*s under excess Zn conditions. The yeast expression vector pKT10 harboring the *AtMTPX* ORF was introduced into BJ5458 *zrc1 cot1* cells carrying pAUR123 (–) or *AtMTP12*-pAUR123 (+). Yeast cells were grown in liquid HC-U medium with antibiotics for 18 h at 30 °C and diluted to 0.1 at D_{660} in the same medium. Aliquots (5 μL) of suspension culture were spotted onto HC-U plates supplemented with various concentrations of $ZnCl_2$. The yeast cells were grown for 2 days at 30 °C and photographed.

C-terminal fragment of YFP (*cYFP*) were fused to the 3′-end of *AtMTP5*s and *AtMTP12*, respectively, and fusion genes were placed downstream of the 35S promoter for transient expression in *A. thaliana* mesophyll protoplasts. In this system, green fluorescence can be observed when the halves of YFP linked to AtMTP12 and AtMTP5s are reconstructed. Mesophyll protoplasts cotransformed with *AtMTP12–cYFP* and *AtMTP5t1–nYFP* plasmids displayed punctate green fluorescence, indicating that these two proteins are capable of forming a heteromer *in vivo* (Fig. 6A). This fluorescence was clearly merged with that of mRFP–SYP31 (*cis*-Golgi) but not with sp-mRFP–HDEL (ER), mRFP–SYP61 (TGN) or mRFP–ARA7 (early endosome), consistent with the results obtained for the AtMTP12–GFP and AtMTP5t1–GFP fusion proteins (Fig. 6A,B). Further observation with ST–mRFP (*trans*-Golgi) showed that AtMTP12/AtMTP5t1 complex-dependent green fluorescence and ST–mRFP-dependent red fluorescence were clearly located side by side with partial overlap (Fig. 6A,C). These results indicate that the AtMTP12/AtMTP5t1 protein complex is localized to the Golgi apparatus. The peak of the fluorescence intensity of YFP in the bimolecular fluorescence complementation assay clearly overlapped with that of mRFP–SYP31 (*cis*-Golgi) (Fig. 6B) rather than ST–mRFP (*trans*-Golgi) (Fig. 6C), suggesting that the AtMTP12/AtMTP5t1 complex resides predominantly in the *cis*-Golgi. Green fluorescence in the Golgi also was observed from mesophyll protoplasts expressing *AtMTP12–cYFP* and *AtMTP5t2–nYFP* (Fig. 6D–F). We confirmed that AtMTP12–cYFP and AtMTP5s–nYFP do not interact with free nYFP and cYFP, respectively (data not shown).

Discussion

AtMTP12 (locus At2g04620) encodes a CDF member with a long N-terminal extension. The aim of this study was to identify this extraordinarily large CDF protein in *A. thaliana* and to determine its Zn transport activity and intracellular localization. The physiological response of AtMTP12 to deficient and excess Zn was also examined.

When AtMTP12 fused with 3HA epitope tags at its C terminus was expressed in *A. thaliana* suspension-cultured cells, the apparent molecular mass of this protein (82.0 kDa) was smaller than predicted (94.7 kDa) (Fig. 1B). This difference raised the possibility that AtMTP12 protein is not synthesized from the putative start codon or cleaved at its N terminus. ZnT5 and Msc2p also reportedly migrate faster than predicted in SDS/PAGE [31,32]. However, the apparent size of the N-terminal truncated (the sequence from 1 to 167, from the first methionine to the second) AtMTP12–3HA was considerably lower than that of AtMTP12–3HA (data not shown). Furthermore, both AtMTP12–GFP and GFP–AtMTP12 were detected in the Golgi apparatus of *A. thaliana* mesophyll protoplasts (data not shown), indicating no post-translational cleavage of the N-terminal part. This study revealed that, in contrast to the other compact AtMTP members, which have six TMs, AtMTP12 is translated as a large protein with 14 TMs.

We examined the effect of Zn concentration on AtMTP12 expression using *A. thaliana* suspension-cultured cells. The amount of AtMTP12–3HA protein was kept constant even under Zn deficient and excess conditions (Fig. 1C,D). It was previously demonstrated that the responses to Zn stress vary among

Fig. 5. Intracellular localization of AtMTP12–GFP and AtMTP5s–GFP in *A. thaliana* protoplasts. AtMTP12–GFP (A), AtMTP5t1–GFP (D) or AtMTP5t2–GFP (E) was transiently expressed in *A. thaliana* mesophyll protoplasts under the control of the CaMV 35S promoter. *mRFP*-tagged intracellular marker genes (ER, *cis*-Golgi, *trans*-Golgi, TGN and early endosome) placed downstream of the CaMV 35S promoter were simultaneously introduced into *A. thaliana* mesophyll protoplasts. Confocal cross-sections show GFP fluorescence (green), mRFP fluorescence (red) and autofluorescence of chlorophyll (Chl, light blue). Merge indicates the overlay of GFP and mRFP fluorescence. Dashed white boxes b and c denote close-up shown in (B) and (C), respectively. The right-hand panels shows the intensity profiles of GFP and mRFP along the line segment *xy* (distance, 2 μm) (B,C). Scale bars = 10 μm.

MTP members. *AtMTP1* is expressed constitutively in the meristem and elongation zone in roots [18,19]. By contrast, *AtMTP3* expression is induced in the epidermis and cortex of the maturation zone in roots under excess Zn conditions [15]. These findings imply that the responsiveness to excess Zn may differ depending on the tissue; namely, precautionary expression of zinc transporters might be important at the root tip for tolerance to excess Zn. Further research is needed to determine the organ, tissue and cell specificity of *AtMTP12* expression.

Here, we note that AtMTP12 and AtMTP5t1 form a heteromeric complex with Zn transport activity. Complementation of the growth defect of the *msc2* mutant was detected only when both AtMTP12 and AtMTP5t1 were present (Fig. 3B). This indicates that AtMTP12, an orthologue of Msc2p, cannot form a functional protein complex with *S. cerevisiae* endogenous Zn transporter Zrg17p, a partner of Msc2p. Based on X-ray crystallography of *Escherichia coli* YiiP, most CDF proteins have been postulated to form homodimers to perform their functions. YiiP was elucidated to function as a Y-shaped homodimer with closely apposed C termini [23]. By contrast, Fukunaka *et al.* [33] clearly demonstrated that ZnT5 and ZnT6 form a heterodimer. They reported that the long N-terminal half of ZnT5 is not important, whereas the cytosolic C-terminal tail is indispensable for the interaction with ZnT6. Their results are consistent with the 3D structure of YiiP. These observations suggest that AtMTP12 and AtMTP5t1 may form a heterodimer. Although AtMTP12 can form a protein complex with not only AtMTP5t1, but also AtMTP5t2 (Fig. 6), the AtMTP12/AtMTP5t2 complex could not complement the *msc2* phenotype (Fig. 3B). In AtMTP5t2, the last 60 amino acids in the C-terminal tail of AtMTP5t1 are missing (Table S1). These results suggest that AtMTP5t1 is a functional variant in *A. thaliana* and that these last 60 amino acid residues are essential for Zn transport activity, but not for the interaction with AtMTP12. In YiiP, four hydrophilic residues in TM2 (Asp45 and Asp49) and TM5 (His153 and Asp157) form a Zn^{2+}-populated site and play a key role during Zn transport [13]. These four hydrophilic residues are conserved in many CDF members (His/Asp and Asp in TM2, His/Asp and Asp in TM5) and have been shown to be essential for Zn transport by site-directed mutagenesis [13,34]. It should be noted that the second residue in TM2 is substituted with glycine in AtMTP5t1 (His146 and Gly150 in TM2, His259 and Asp263 in TM5), although AtMTP12 has four conserved residues (His452 and Asp456 in TM10, His662 and Asp666 in TM13). Human and yeast orthologues of AtMTP12 also harbor four conserved residues, but orthologues of AtMTP5t1 do not. Therefore, a lack of Zn^{2+}-binding residues in the partner protein of AtMTP12 orthologues may be common in a wide variety of species. AtMTP5t1 is unlikely to transport Zn, but is essential for the Zn transport activity of AtMTP12. Further study to determine kinetic properties such as K_m and V_{max} is necessary to understand the physiological role of the AtMTP12/AtMTP5t1 complex in the Golgi apparatus. Ohana *et al.* [35] reported that the ZnT5/ZnT6 complex functions as a Zn^{2+}/H^+ antiporter.

Determining the intracellular localization of AtMTP12 and AtMTP5t1 was the key objective of this study. To date, the intracellular localization of the AtMTP12 and AtMTP5t1 orthologues in other organisms has been determined individually. Orthologues in *S. cerevisiae* (Msc2p and Zrg17p) are localized to the ER, and in *S. pombe* (Cis4) to the *cis*-Golgi [28,30,36]. *Homo sapiens* ZnT5 and ZnT6 are localized to the Golgi apparatus [33,37]. Another report indicated that ZnT5 is concentrated in the early secretory pathway such as COPII-coated vesicles and the Golgi apparatus [38]. This study clearly demonstrated the intracellular localization of CDF proteins AtMTP12 and AtMTP5t1 in the Golgi apparatus as a complex. Moreover, this complex is estimated to be localized predominantly in the *cis*-Golgi (Fig. 6A–C). It should be noted that the transient expression of a GFP fusion protein indicated that AtMTP5t1 might be localized to both the *cis*- and *trans*-Golgi in spite of the *cis*-Golgi localization of AtMTP12 (Fig. 5). One intriguing aspect of the intracellular localization of these proteins is whether the localization of AtMTP5t1 is AtMTP12 dependent; namely, whether AtMTP12 is required for

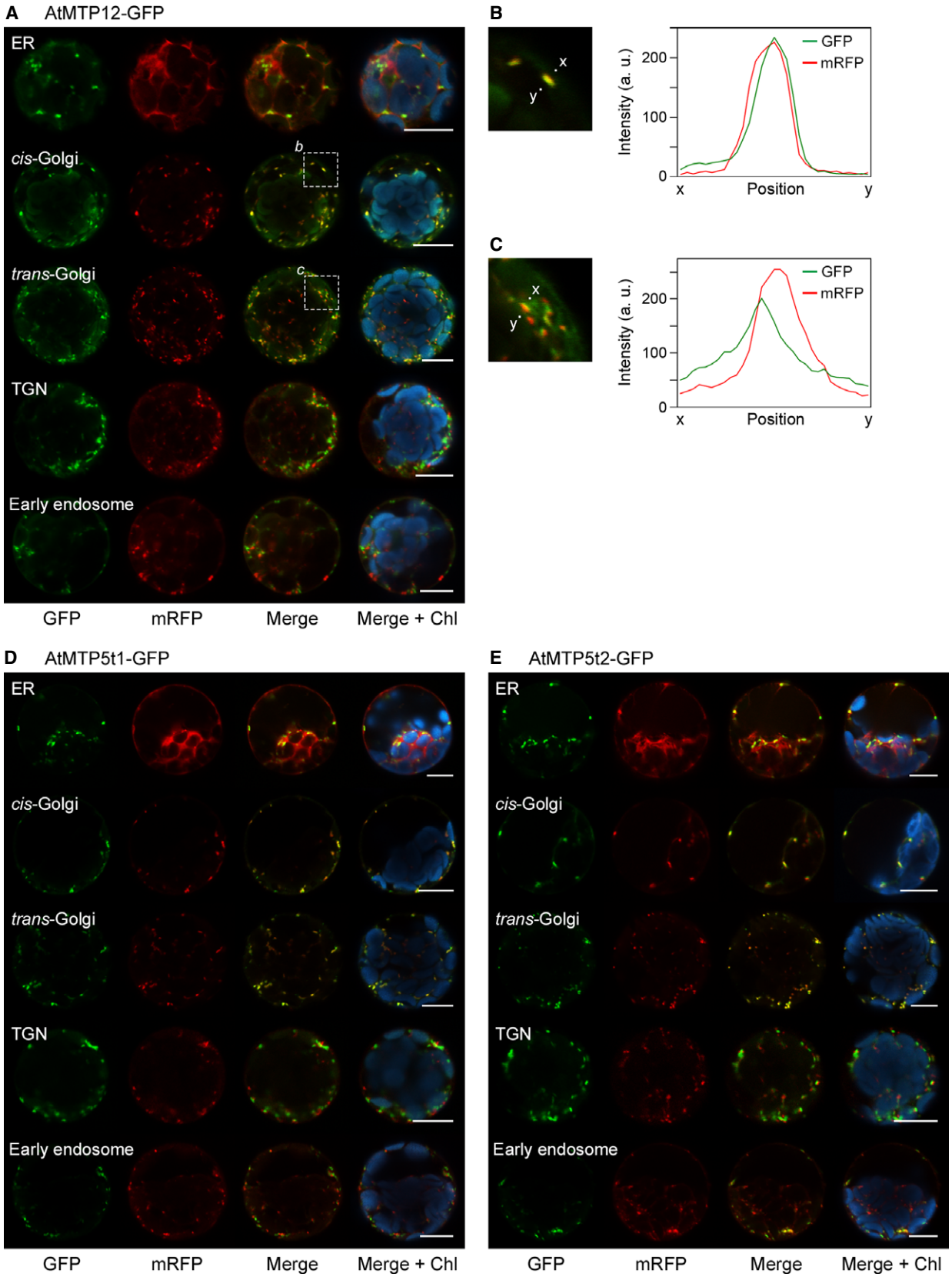
A
AtMTP12-GFP
ER
cis-Golgi
trans-Golgi
TGN
Early endosome
b
c
GFP
mRFP
Merge
Merge + Chl
B
x
y
Intensity (a. u.)
200
100
0
Position
C
D
AtMTP5t1-GFP
E
AtMTP5t2-GFP

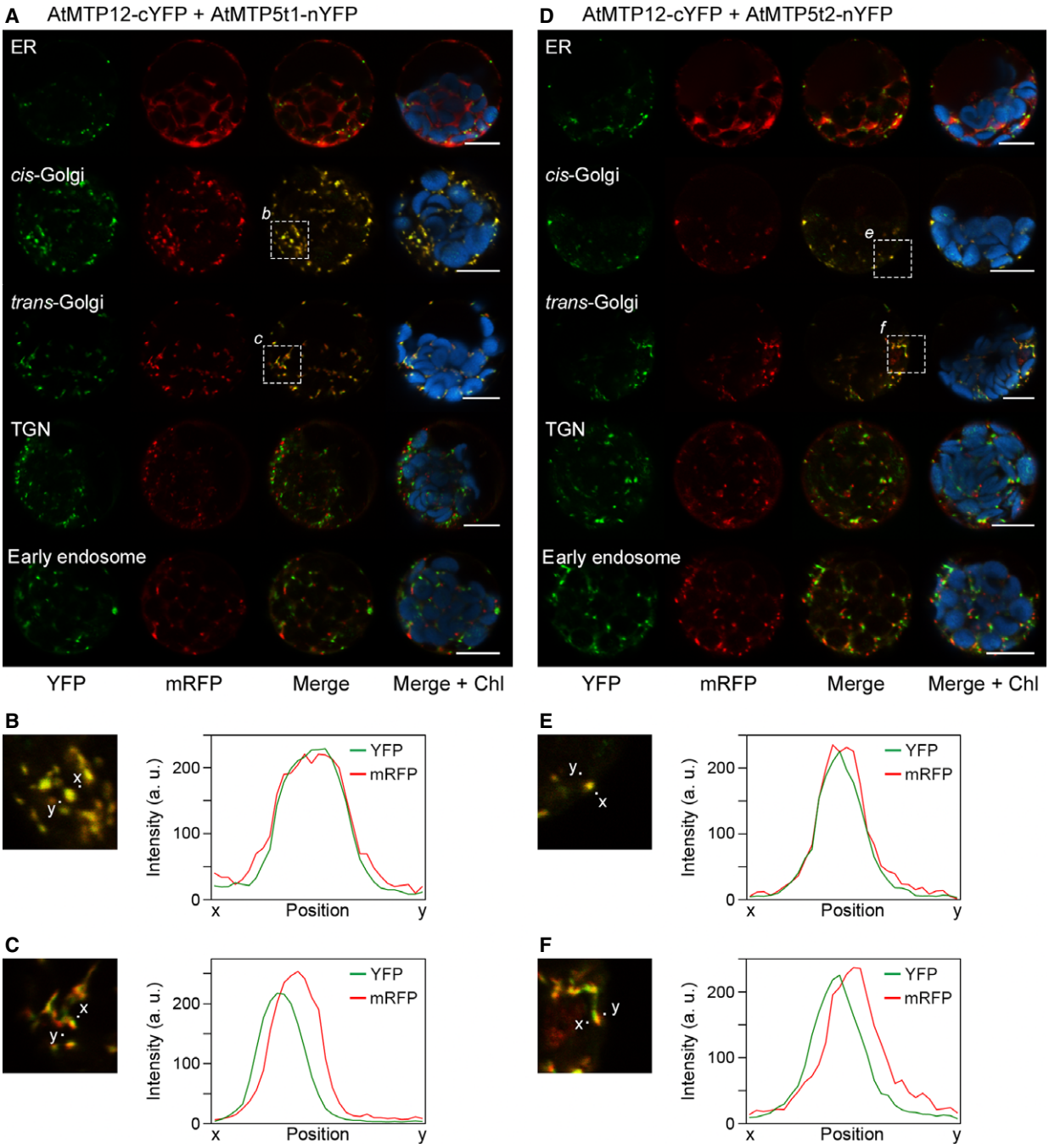

Fig. 6. Bimolecular fluorescence complementation assays for heterooligomerization of AtMTP12 and AtMTP5s. *AtMTP12–cYFP* and *AtMTP5t1–nYFP* (A) or *AtMTP12–cYFP* and *AtMTP5t2–nYFP* (D) were coexpressed in *A. thaliana* mesophyll protoplasts under the control of the CaMV 35S promoter. *mRFP*-tagged intracellular marker genes were simultaneously introduced. Fluorescence of reconstructed YFP, mRFP and chlorophyll are shown in green, red and light blue, respectively. Merge indicates the overlay of YFP and mRFP fluorescence. Dashed white boxes b, c, e and f denote close-up shown in (B), (C), (E) and (F), respectively. The right-hand panels shows the intensity profiles of YFP and mRFP along the line segment *xy* (distance, 2 μm) (B,C,E,F). Scale bars = 10 μm.

cis-Golgi localization of AtMTP5t1. In some plants, plasma membrane intrinsic protein 1 (PIP1), an aquaporin, fails to reach the plasma membrane in the absence of PIP2 [39]. PIP1–PIP2 interaction might be indispensable for PIP1 trafficking to the plasma membrane. Taking into consideration that most MTP

members from stable dimers, as demonstrated for YiiP, we speculate that AtMTP5t1 usually forms a complex with AtMTP12 just after translation in the ER and then is recruited to the *cis*-Golgi.

The functions of CDF members have been examined by heterologous expression in metal-hypersensitive yeast mutants. Their Zn transport functions have been inferred by demonstrating increased tolerance of transformed yeast cells to excess Zn. Here, we discuss the biochemical and intracellular properties of AtMTP members. In the case of AtMTP12, the *zrc1 cot1* double-mutant phenotype was not complemented by AtMTP12 even in the presence of AtMTP5t1 (Fig. 4). We first predicted that Zn is sequestered into the Golgi apparatus by the AtMTP12/AtMTP5t1 complex and then transported to the vacuole or released from the cell via exocytosis. The results obtained suggest that Zn sequestering into the Golgi is insufficient to reduce the concentration of Zn^{2+} in the cytosol under excess Zn conditions. By contrast, it was demonstrated that AtMTP11, which belongs to a different phylogenetic subgroup of CDF proteins, is localized at the *trans*-Golgi and can confer tolerance to excess Mn when expressed in Mn-hypersensitive yeast cells [21]. However, another group reported that AtMTP11 is localized to the pre-vacuolar compartment [20]. We showed that the *zrc1 cot1* double-mutants expressing vacuolar-localized Zn transporters such as AtMTP1 and AtMTP3 grow under excess Zn conditions, as reported previously [15,16]. In addition to AtMTP1 and AtMTP3, we also found that yeast cells expressing AtMTP2 or AtMTP4 were able to grow in medium supplemented with excess Zn. These results suggested a cellular function for these transporters in the detoxification of Zn by preventing its intracellular accumulation or sequestering it into an intracellular compartment. Furthermore, AtMTP3t1 conferred a lower tolerance to excess Zn to the double-mutant than to AtMTP3t2. In AtMTP3t1, 39 amino acids are inserted in the N-terminal tail, so it has a longer N-terminal tail than AtMTP3t2. It can be speculated that this region has changed the transport activity of AtMTP3t1 (Table S1).

Our findings strongly suggested that AtMTP12 forms a heteromeric complex with AtMTP5t1 to transport Zn into the Golgi apparatus, probably *cis*-Golgi. Both *AtMTP12* and *AtMTP5* are expressed in leaves, flowers and roots, according to an open database on an *Arabidopsis* eFP browser [40]. Thus, we predict that the AtMTP12/AtMTP5t1 complex supplies Zn to the Zn-requiring proteins that reside in the Golgi apparatus in cells of these organs. Recent research has brought important advances in our understanding of the role of Zn transporters in the secretory pathway. In *H. sapiens*, the ZnT5/ZnT6 complex and another Golgi-localized Zn transporter, ZnT7, supply Zn to tissue-nonspecific alkaline phosphatase, which is transported from the Golgi apparatus to the plasma membrane through the secretory pathway [38,41]. In *S. cerevisiae*, Msc2p/Zrg17p are required for ER function [28,36]. Furthermore, Cis4 has been implicated in maintaining the membrane-trafficking function in *S. pombe* [30]. However, no information on the molecular system or physiological role of Zn transporters in the secretory pathway of plants is available. Our findings may provide us with a novel point of view concerning the requirement for Zn in the Golgi apparatus that is provided by AtMTP12/AtMTP5t1 in plants.

Experimental procedures

Plant materials, growth conditions and transformation

Arabidopsis thaliana suspension-cultured T87 cells (background strain Columbia) [42] were cultured in modified LS medium [43] at 22 °C with rotary shaking at 120 r.p.m. under dark conditions. Cells cultivated for 7 days were filtered through a 500-μm stainless sieve and 5 mL of sieved cells was added to a 300 mL Erlenmeyer flask containing 95 mL of fresh modified LS medium for subculture. Stable transformation of T87 cells by cocultivation with *Agrobacterium tumefaciens* was performed as described previously with the modifications described below [44]. *Agrobacterium tumefaciens* strain C58C1 (pMP90) [45] carrying a binary vector was added to a 2-day-old precultured T87 cell suspension. After cocultivation for 2 days, claforan (500 $mg \cdot L^{-1}$) (Sanofi, Tokyo, Japan) was added to arrest bacterial growth and T87 cells were cultured for a further 3 days. Subculture was performed as described above in modified LS medium containing 10 $mg \cdot L^{-1}$ hygromycin as well as claforan. For Zn stress treatment, 5-day-old transformed T87 cells were collected by centrifugation at 100 ***g*** for 1 min at 22 °C. After washing three times in modified LS medium in which Zn was omitted, cells were resuspended in modified LS medium containing various concentrations of $ZnSO_4$ or 5 μM *N*,*N*,*N*′,*N*′-tetrakis(2-pyridylmethyl)ethylenediamine, a Zn chelator, and incubated for a maximum of 2 days.

Cloning of *AtMTP12*

Full-length *AtMTP12* cDNA (DDBJ accession number, **AB986953**) was obtained by 5′- and 3′-RACE based on a partial sequence of *AtMTP12* cDNA in the database of

TAIR. Briefly, total RNA was extracted from 3-week-old whole plants of *A. thaliana* strain Columbia-0 using an RNeasy Mini Kit (Qiagen, Valencia, CA, USA). 5′- and 3′-RACE PCRs were performed with total RNA using a GeneRacer Kit (Life Technologies, Carlsbad, CA, USA). All primers used in this study are shown in Table S2. The resulting PCR products were cloned into the pCR-Blunt vector (Life Technologies) and verified by sequencing.

Expression analysis of AtMTP12–3HA in transgenic T87 cells

Genomic DNA was extracted from 3-week-old whole plants of *A. thaliana* strain Columbia-0 using a DNeasy Plant Mini Kit (Qiagen). The pBI121 vector [46] was digested with *Hin*dIII and *Eco*RI. The fragment obtained, containing the CaMV 35S promoter, β-glucuronidase and nopaline synthase terminator (NosT), was ligated into the *Hin*dIII–*Eco*RI site of pCAMBIA1300 vector (Cambia, Canberra, Australia) to produce pCAMBIA35N vector. To fuse 3HA epitope tags in frame to the 3′-end of coding region of *AtMTP12*, a four-round PCR was carried out. In the first round, a genomic DNA fragment of the *AtMTP12* promoter followed by the ORF of *AtMTP12* (–3124 bp from the start codon to the end of the ORF without a stop codon) was amplified. The resulting PCR product was further amplified three times using the same forward primer and three overlapping reverse primers. The fragment obtained was inserted into the *Pst*I–*Sac*I site of pCAMBIA35N with a replacement of the fragment containing CaMV 35S promoter and β-glucuronidase and fully sequenced to confirm that no modifications had occurred. *Agrobacterium tumefaciens* strain C58C1 (pMP90) was transformed with the resulting plasmid and pCAMBIA35N by electroporation [47] and then introduced to T87 cells as described above.

Crude membrane preparation and immunoblotting

To prepare crude membrane fractions, transformed T87 cells were harvested on a 40 μm nylon mesh (Millipore, Billerica, MA, USA) by filtration, frozen by liquid nitrogen and homogenized in liquid nitrogen using a mortar and pestle. The lysed cells were suspended in a 10-fold volume of extraction buffer containing 50 mM Tris/HCl (pH 8.0), 2 mM EDTA, 20% (v/v) glycerol, 1 mM dithiothreitol and 2× Complete protease inhibitor cocktail (Roche Applied Science, Mannheim, Germany). The suspension was centrifuged at 10 000 ***g*** for 10 min at 4 °C to remove any cell debris. After centrifugation of the supernatant at 146 000 ***g*** for 40 min at 4 °C, the precipitate obtained was resuspended in extraction buffer. SDS/PAGE and immunoblotting were carried out as described previously with the modifications as described below [34]. The membrane was incubated with monoclonal anti-HA Ig (Nacalai Tesque, Kyoto, Japan) at a dilution of 1 : 40 000 and then with anti-mouse IgG conjugated with horseradish peroxidase (GE Healthcare, Piscataway, NJ, USA) at a dilution of 1 : 200 000 in Can Get Signal Immunoreaction Enhancer Solution (Toyobo, Osaka, Japan). A SuperSignal West Femto chemiluminescent kit (Thermo Scientific, Rockford, IL, USA) was used to detect antigens.

Growth Assay of *S. cerevisiae* mutants

A DNA fragment containing the *GAL1* promoter and *CYC1* terminator was amplified by PCR using pYES2 vector (Life Technologies) as a template. The region from the *ADH1* promoter to the *ADH1* terminator of pAUR123 vector (Takara Bio, Otsu, Japan) was replaced with this PCR-amplified fragment via the *Bam*HI sites to generate pAUR123GAL1 vector. The *AtMTP12* ORF was amplified and ligated into the pKT10 (*Eco*RI–*Sal*I site) [48], pAUR123GAL1 (*Kpn*I–*Xba*I site) and pAUR123 (*Kpn*I–*Xba*I site) vectors. In addition, the ORFs of the other MTP members from *A. thaliana* (Table S1) were amplified and cloned into the pYES2 (*Kpn*I–*Eco*RI or *Kpn*I–*Xba*I site) and pKT10 (*Eco*RI–*Kpn*I or *Kpn*I–*Sal*I site) vectors. For genes predicted to have alternative splicing variants, all variants were isolated or synthesized based on cDNA sequence in TAIR (Table S1). Furthermore, the *MSC2* ORF was amplified by colony PCR from *S. cerevisiae* strain DY150 (*MATa ade2 can1 his3 leu2 trp1 ura3*) [31,49] and cloned into the *Sac*I–*Xho*I site of pAUR123GAL1 and pYES2 vectors. Sequencing confirmed the accuracy of all the PCR-amplified fragments. The *S. cerevisiae* mutants DY150 *msc2* (DY150 *msc2::HIS3*) [31] and BJ5458 *zrc1 cot1* (*MATα ura3–52 trp1 lys2–801 leu2Δ1 his3Δ200 pep4::HIS3 prb1Δ1.6R can1 GAL zrc1::LEU2 cot1::TRP1*) [16] were transformed with the plasmids obtained using a lithium acetate/single-stranded carrier DNA/polyethylene glycol method [50]. For the DY150 *msc2* mutant, transformants were selected on solid synthetic dextrose medium [51] with appropriate amino acids for auxotrophy and 500 $\mu g \cdot mL^{-1}$ aureobasidin A (Takara Bio) at 30 °C. Then, the transformed yeast cells were precultured in SRaf medium (synthetic dextrose medium containing 2% w/v raffinose instead of 2% w/v glucose) with appropriate amino acids and aureobasidin A for 18 h at 30 °C. These cultures were subsequently diluted to $D_{660} = 0.1$ in SGal medium (synthetic dextrose medium containing 2% w/v galactose instead of 2% w/v glucose) with appropriate amino acids. After incubation at 30 °C for 1 h, 5 μL of culture was spotted onto solid YPGEgal medium [28] supplemented with various concentrations of $ZnSO_4$. Plates were incubated for 3 days at 30 or 37 °C. For the BJ5458 *zrc1 cot1* mutant, transformants were selected on solid HC-U medium [16] at 30 °C. The desired yeast cells were grown in

HC-U medium for 18 h at 30 °C and subsequently diluted to D_{660} = 0.1 in the same medium. Aureobasidin A was added to the HC-U medium for the yeast cells transformed with pAUR123 vector. Aliquots (5 μL) were spotted onto solid HC-U medium supplemented with various concentrations of $ZnCl_2$. Plates were incubated for 2 days at 30 °C.

Transient expression of fusion proteins in *A. thaliana* mesophyll protoplasts

The ORFs of *AtMTP12* and *AtMTP5*s were fused to the ORF of *GFP* [52] in the 5′-*AtMTPX-GFP*-3′ and 5′-*GFP-AtMTPX*-3′ directions by PCR fusion ('X' indicates family member number). For example, to generate *AtMTP12–GFP*, the ORFs of *AtMTP12* and *GFP* were amplified by PCR using the primer pairs TR1/TR2 and TR6/TR7, respectively (Table S2). The two PCR products were mixed and amplified using the primers TR1 and TR7. The resulting PCR product was inserted into the *Xba*I–*Sac*I site of pCAMBIA35N. The same approach was applied to the construction of the other plasmids. For bimolecular fluorescence complementation assays, the DNA fragment containing *nYFP* followed by NosT was amplified by PCR using pGWnY vector as a template; a parallel amplification was carried out with the *cYFP* followed by NosT using pGWcY vector as a template [52,53]. PCR fusions were performed as described above to generate *AtMTP5*s–*nYFP*:NosT and *AtMTP12–cYFP*:NosT; these PCR products were ligated into the *Xba*I–*Eco*RI site of pnYGW and pCAMBIA35N vectors, respectively. All constructs were verified by sequencing. Plasmids containing *sp-mRFP–HDEL* [52,54], *mRFP–SYP31* [55], *ST–mRFP* [56], *mRFP–SYP61* [55] and *mRFP–ARA7* [57] placed downstream of the 35S promoter were used as intracellular markers of ER, *cis*-Golgi, *trans*-Golgi, TGN and early endosome, respectively. Transient gene expression in the *A. thaliana* mesophyll protoplasts was carried out as previously described [58]. Green and red fluorescence was observed by FV1000-D confocal laser scanning microscope (Olympus, Tokyo, Japan). Intensity profiling of fluorescence levels were performed using IMAGEJ software [59].

Acknowledgements

We are grateful to Dr Takashi Ueda (The University of Tokyo, Japan) for valuable discussions and providing cDNAs encoding intracellular markers (*cis*-Golgi, *trans*-Golgi, TGN, and early endosome). We also thank Dr David Eide (University of Wisconsin-Madison, USA), Dr Tsuyoshi Nakagawa (Shimane University, Japan) and Dr Ikuko Hara-Nishimura (Kyoto University, Japan) for providing *S. cerevisiae* strains (DY150 and DY150 *msc2*), bimolecular fluorescence complementation vectors (pGWnY, pGWcY, and pnYGW), and cDNA encoding an ER marker, respectively. TF received Research Fellowships of the Japan Society for the Promotion of Science for Young Scientists. This work was supported by Grants-in-Aid from the Ministry of Education, Culture, Sports, Science and Technology of Japan to TF (50724499) NK (24770038) and MM (25650093 and 26252011) and from the Steel Foundation for Environmental Protection Technology (2010-29) to M. M.

Author contributions

TF, MK and MM planned the experiments and wrote the article. TF, YS and HM performed the experiments and analyzed data. NK and SH analyzed the data.

References

1 Sinclair SA & Krämer U (2012) The zinc homeostasis network of land plants. *Biochim Biophys Acta* **1823**, 1553–1567.
2 Krämer U & Clemens S (2006) Functions and homeostasis of zinc, copper, and nickel in plants. In Molecular Biology of Metal Homeostasis and Detoxification (Tamás MJ & Martinoia E, eds), pp. 215–272. Springer, Berlin.
3 Grotz N, Fox T, Connolly E, Park W, Guerinot ML & Eide D (1998) Identification of a family of zinc transporter genes from *Arabidopsis* that respond to zinc deficiency. *Proc Natl Acad Sci USA* **95**, 7220–7224.
4 Korshunova YO, Eide D, Clark WG, Guerinot ML & Pakrasi HB (1999) The IRT1 protein from *Arabidopsis thaliana* is a metal transporter with a broad substrate range. *Plant Mol Biol* **40**, 37–44.
5 Lin YF, Liang HM, Yang SY, Boch A, Clemens S, Chen CC, Wu JF, Huang JL & Yeh KC (2009) Arabidopsis IRT3 is a zinc-regulated and plasma membrane localized zinc/iron transporter. *New Phytol* **182**, 392–404.
6 Vert G, Barberon M, Zelazny E, Séguéla M, Briat JF & Curie C (2009) *Arabidopsis* IRT2 cooperates with the high-affinity iron uptake system to maintain iron homeostasis in root epidermal cells. *Planta* **229**, 1171–1179.
7 Milner MJ, Seamon J, Craft E & Kochian LV (2013) Transport properties of members of the ZIP family in plants and their role in Zn and Mn homeostasis. *J Exp Bot* **64**, 369–381.
8 Vert G, Briat JF & Curie C (2001) *Arabidopsis IRT2* gene encodes a root-periphery iron transporter. *Plant J* **26**, 181–189.

9 Hussain D, Haydon MJ, Wang Y, Wong E, Sherson SM, Young J, Camakaris J, Harper JF & Cobbett CS (2004) P-type ATPase heavy metal transporters with roles in essential zinc homeostasis in Arabidopsis. *Plant Cell* **16**, 1327–1339.
10 Sinclair SA, Sherson SM, Jarvis R, Camakaris J & Cobbett CS (2007) The use of the zinc-fluorophore, Zinpyr-1, in the study of zinc homeostasis in *Arabidopsis* roots. *New Phytol* **174**, 39–45.
11 Verret F, Gravot A, Auroy P, Leonhardt N, David P, Nussaume L, Vavasseur A & Richaud P (2004) Overexpression of AtHMA4 enhances root-to-shoot translocation of zinc and cadmium and plant metal tolerance. *FEBS Lett* **576**, 306–312.
12 Morel M, Crouzet J, Gravot A, Auroy P, Leonhardt N, Vavasseur A & Richaud P (2009) AtHMA3, a P_{1B}-ATPase allowing Cd/Zn/Co/Pb vacuolar storage in Arabidopsis. *Plant Physiol* **149**, 894–904.
13 Montanini B, Blaudez D, Jeandroz S, Sanders D & Chalot M (2007) Phylogenetic and functional analysis of the Cation Diffusion Facilitator (CDF) family: improved signature and prediction of substrate specificity. *BMC Genom* **8**, 107.
14 Kobae Y, Uemura T, Sato MH, Ohnishi M, Mimura T, Nakagawa T & Maeshima M (2004) Zinc transporter of *Arabidopsis thaliana* AtMTP1 is localized to vacuolar membranes and implicated in zinc homeostasis. *Plant Cell Physiol* **45**, 1749–1758.
15 Arrivault S, Senger T & Krämer U (2006) The Arabidopsis metal tolerance protein AtMTP3 maintains metal homeostasis by mediating Zn exclusion from the shoot under Fe deficiency and Zn oversupply. *Plant J* **46**, 861–879.
16 Kawachi M, Kobae Y, Mimura T & Maeshima M (2008) Deletion of a histidine-rich loop of AtMTP1, a vacuolar Zn^{2+}/H^{+} antiporter of *Arabidopsis thaliana*, stimulates the transport activity. *J Biol Chem* **283**, 8374–8383.
17 Dräger DB, Desbrosses-Fonrouge AG, Krach C, Chardonnens AN, Meyer RC, Saumitou-Laprade P & Krämer U (2004) Two genes encoding *Arabidopsis halleri* MTP1 metal transport proteins co-segregate with zinc tolerance and account for high *MTP1* transcript levels. *Plant J* **39**, 425–439.
18 Desbrosses-Fonrouge AG, Voigt K, Schröder A, Arrivault S, Thomine S & Krämer U (2005) *Arabidopsis thaliana* MTP1 is a Zn transporter in the vacuolar membrane which mediates Zn detoxification and drives leaf Zn accumulation. *FEBS Lett* **579**, 4165–4174.
19 Kawachi M, Kobae Y, Mori H, Tomioka R, Lee Y & Maeshima M (2009) A mutant strain *Arabidopsis thaliana* that lacks vacuolar membrane zinc transporter MTP1 revealed the latent tolerance to excessive zinc. *Plant Cell Physiol* **50**, 1156–1170.
20 Delhaize E, Gruber BD, Pittman JK, White RG, Leung H, Miao Y, Jiang L, Ryan PR & Richardson AE (2007) A role for the *AtMTP11* gene of Arabidopsis in manganese transport and tolerance. *Plant J* **51**, 198–210.
21 Peiter E, Montanini B, Gobert A, Pedas P, Husted S, Maathuis FJM, Blaudez D, Chalot M & Sanders D (2007) A secretory pathway-localized cation diffusion facilitator confers plant manganese tolerance. *Proc Natl Acad Sci USA* **104**, 8532–8537.
22 Tanaka N, Kawachi M, Fujiwara T & Maeshima M (2013) Zinc-binding and structural properties of the histidine-rich loop of *Arabidopsis thaliana* vacuolar membrane zinc transporter MTP1. *FEBS Open Bio* **3**, 218–224.
23 Lu M & Fu D (2007) Structure of the zinc transporter YiiP. *Science* **317**, 1746–1748.
24 Gupta S, Chai J, Cheng J, D'Mello R, Chance MR & Fu D (2014) Visualizing the kinetic power stroke that drives proton-coupled zinc(II) transport. *Nature* **512**, 101–104.
25 Becher M, Talke IN, Krall L & Krämer U (2004) Cross-species microarray transcript profiling reveals high constitutive expression of metal homeostasis genes in shoots of the zinc hyperaccumulator *Arabidopsis halleri*. *Plant J* **37**, 251–268.
26 Kamizono A, Nishizawa M, Teranishi Y, Murata K & Kimura A (1989) Identification of a gene conferring resistance to zinc and cadmium ions in the yeast *Saccharomyces cerevisiae*. *Mol Gen Genet* **219**, 161–167.
27 Conklin DS, McMaster JA, Culbertson MR & Kung C (1992) *COT1*, a gene involved in cobalt accumulation in *Saccharomyces cerevisiae*. *Mol Cell Biol* **12**, 3678–3688.
28 Ellis CD, MacDiarmid CW & Eide DJ (2005) Heteromeric protein complexes mediate zinc transport into the secretory pathway of eukaryotic cells. *J Biol Chem* **280**, 28811–28818.
29 Suzuki T, Ishihara K, Migaki H, Ishihara K, Nagao M, Yamaguchi-Iwai Y & Kambe T (2005) Two different zinc transport complexes of cation diffusion facilitator proteins localized in the secretory pathway operate to activate alkaline phosphatases in vertebrate cells. *J Biol Chem* **280**, 30956–30962.
30 Fang Y, Sugiura R, Ma Y, Yada-Matsushima T, Umeno H & Kuno T (2008) Cation diffusion facilitator Cis4 is implicated in Golgi membrane trafficking via regulating zinc homeostasis in fission yeast. *Mol Biol Cell* **19**, 1295–1303.
31 Li L & Kaplan J (2001) The yeast gene *MSC2*, a member of the cation diffusion facilitator family, affects the cellular distribution of zinc. *J Biol Chem* **276**, 5036–5043.
32 Kambe T, Narita H, Yamaguchi-Iwai Y, Hirose J, Amano T, Sugiura N, Sasaki R, Mori K, Iwanaga T &

Nagao M (2002) Cloning and characterization of a novel mammalian zinc transporter, zinc transporter 5, abundantly expressed in pancreatic β cells. *J Biol Chem* **277**, 19049–19055.
33 Fukunaka A, Suzuki T, Kurokawa Y, Yamazaki T, Fujiwara N, Ishihara K, Migaki H, Okumura K, Masuda S, Yamaguchi-Iwai Y *et al.* (2009) Demonstration and characterization of the heterodimerization of ZnT5 and ZnT6 in the early secretory pathway. *J Biol Chem* **284**, 30798–30806.
34 Kawachi M, Kobae Y, Kogawa S, Mimura T, Krämer U & Maeshima M (2012) Amino acid screening based on structural modeling identifies critical residues for the function, ion selectivity and structure of Arabidopsis MTP1. *FEBS J* **279**, 2339–2356.
35 Ohana E, Hoch E, Keasar C, Kambe T, Yifrach O, Hershfinkel M & Sekler I (2009) Identification of the Zn^{2+} binding site and mode of operation of a mammalian Zn^{2+} transporter. *J Biol Chem* **284**, 17677–17686.
36 Ellis CD, Wang F, MacDiarmid CW, Clark S, Lyons T & Eide DJ (2004) Zinc and the Msc2 zinc transporter protein are required for endoplasmic reticulum function. *J Cell Biol* **166**, 325–335.
37 Huang L, Kirschke CP & Gitschier J (2002) Functional characterization of a novel mammalian zinc transporter, ZnT6. *J Biol Chem* **277**, 26389–26395.
38 Suzuki T, Ishihara K, Migaki H, Matsuura W, Kohda A, Okumura K, Nagao M, Yamaguchi-Iwai Y & Kambe T (2005) Zinc transporters, ZnT5 and ZnT7, are required for the activation of alkaline phosphatases, zinc-requiring enzymes that are glycosylphosphatidylinositol-anchored to the cytoplasmic membrane. *J Biol Chem* **280**, 637–643.
39 Chaumont F & Tyerman SD (2014) Aquaporins: highly regulated channels controlling plant water relations. *Plant Physiol* **164**, 1600–1618.
40 Winter D, Vinegar B, Nahal H, Ammar R, Wilson GV & Provart NJ (2007) An "Electronic Fluorescent Pictograph" browser for exploring and analyzing large-scale biological data sets. *PLoS One* **2**, e718.
41 Kirschke CP & Huang L (2003) ZnT7, a novel mammalian zinc transporter, accumulates zinc in the Golgi apparatus. *J Biol Chem* **278**, 4096–4102.
42 Axelos M, Curie C, Mazzolini L, Bardet C & Lescure B (1992) A protocol for transient gene expression in *Arabidopsis thaliana* protoplasts isolated from cell-suspension cultures. *Plant Physiol Biochem* **30**, 123–128.
43 Nagata T, Okada K, Takebe I & Matsui C (1981) Delivery of tobacco mosaic virus RNA into plant protoplasts mediated by reverse-phase evaporation vesicles (Liposomes). *Mol Gen Genet* **184**, 161–165.
44 Ferrando A, Farràs R, Jásik J, Schell J & Koncz C (2000) Intron-tagged epitope: a tool for facile detection and purification of proteins expressed in *Agrobacterium*-transformed plant cells. *Plant J* **22**, 553–560.
45 Koncz C & Schell J (1986) The promoter of T_L-DNA gene *5* controls the tissue-specific expression of chimeric genes carried by a novel type of *Agrobacterium* binary vector. *Mol Gen Genet* **204**, 383–396.
46 Chen PY, Wang CK, Soong SC & To KY (2003) Complete sequence of the binary vector pBI121 and its application in cloning T-DNA insertion from transgenic plants. *Mol Breed* **11**, 287–293.
47 Shen WJ & Forde BG (1989) Efficient transformation of *Agrobacterium* spp. by high voltage electroporation. *Nucleic Acids Res* **17**, 8385.
48 Tanaka K, Nakafuku M, Tamanoi F, Kaziro Y, Matsumoto K & Toh-e A (1990) *IRA2*, a second gene of *Saccharomyces cerevisiae* that encodes a protein with a domain homologous to mammalian *ras* GTPase-activating protein. *Mol Cell Biol* **10**, 4303–4313.
49 Akada R, Murakane T & Nishizawa Y (2000) DNA extraction method for screening yeast clones by PCR. *Biotechniques* **28**, 668–674.
50 Gietz RD & Woods RA (2002) Transformation of yeast by lithium acetate/single-stranded carrier DNA/polyethylene glycol method. *Methods Enzymol* **350**, 87–96.
51 Rose MD, Winston F & Hieter P (1990) Methods In Yeast Genetics: A Laboratory Course Manual. Cold Spring Harbor Laboratory Press, Cold Spring Harbor, NY.
52 Müller-Taubenberger A & Anderson KI (2007) Recent advances using green and red fluorescent protein variants. *Appl Microbiol Biotechnol* **77**, 1–12.
53 Hino T, Tanaka Y, Kawamukai M, Nishimura K, Mano S & Nakagawa T (2011) Two Sec13p homologs, AtSec13A and AtSec13B, redundantly contribute to the formation of COPII transport vesicles in *Arabidopsis thaliana*. *Biosci Biotechnol Biochem* **75**, 1848–1852.
54 Tamura K, Shimada T, Kondo M, Nishimura M & Hara-Nishimura I (2005) KATAMARI1/MURUS3 is a novel golgi membrane protein that is required for endomembrane organization in Arabidopsis. *Plant Cell* **17**, 1764–1776.
55 Uemura T, Ueda T, Ohniwa RL, Nakano A, Takeyasu K & Sato MH (2004) Systematic analysis of SNARE molecules in *Arabidopsis*: dissection of the post-Golgi network in plant cells. *Cell Struct Funct* **29**, 49–65.
56 Ito Y, Uemura T, Shoda K, Fujimoto M, Ueda T & Nakano A (2012) *cis*-Golgi proteins accumulate near the ER exit sites and act as the scaffold for Golgi regeneration after brefeldin A treatment in tobacco BY-2 cells. *Mol Biol Cell* **23**, 3203–3214.

57 Ueda T, Uemura T, Sato MH & Nakano A (2004) Functional differentiation of endosomes in Arabidopsis cells. *Plant J* **40**, 783–789.
58 Yoo SD, Cho YH & Sheen J (2007) *Arabidopsis* mesophyll protoplasts: a versatile cell system for transient gene expression analysis. *Nat Protoc* **2**, 1565–1572.
59 Abràmoff MD, Magalhães PJ & Ram SJ (2004) Image processing with ImageJ. *Biophotonics Int* **11**, 36–42.

Supporting information

Additional supporting information may be found in the online version of this article at the publisher's web site:
Table S1. AGI codes of AtMTPs.
Table S2. Primers used in this research.